International Journal of Automotive Research, Vol. 9, No. 1, (2019), 2895-2907

Iran University of Science and Technology

International Journal of Automotive Engineering

Journal Homepage: ijae.iust.ac.ir

ISSN: 2008-6989

An adaptive modified fuzzy-sliding mode longitudinal control design and simulation for vehicles equipped with ABS system

Sina Sadeghi Namaghi[1], Majid Moavenian[*]

[1]MSc student, Mechanic Department of Ferdowsi University of Mashhad, Mashhad, Iran

[*]Associate Professor, Mechanic Department of Ferdowsi University of Mashhad, Mashhad, Iran

ARTICLE INFO

Article history:

Received : 26 Feb 2019

Accepted: 18 Mar 2019

Published:

Keywords:

ABS

Adaptive Fuzzy-PID

SMC

Longitudinal Stability

A B S T R A C T

In order to improve the safety and longitudinal stability of a vehicle equipped with standard ABS system, this paper, analyzes the basic principles of vehicles stability and proposes a control strategy based on fuzzy adaptive control which will adjust PID gain parameters, using genetic algorithm. A linear three-degree-of-freedom (DOF) vehicle model was set up in Simulink and the stability test was conducted utilizing jointly a joint established simulation platform with CarSim. For controlling the brake length, traditional controllers have difficulty in guaranteeing performance and stability over a wide range of parameter changes and disturbances. Therefore, a two level controller by providing a modified Sliding Mode Control (SMC) will be used. Using this approach the flexibility increased and brake length and rotor temperatures decreases significantly. This results improvement of the vehicle's stability and brakes fatigue lifespan.

1. Introduction

When a vehicle is travelling at high speeds and brakes are applied, the wheels are the first to slow down. But the vehicle itself continues to travel by its own momentum which is higher than the wheels due to higher unsprung mass of the vehicle. Hence the vehicle does not slow down as quickly as the wheels. This difference in speed causes the wheels to lock up. In such a case the driver has no control over the steering and hence the direction of the vehicle cannot be controllable. This causes many accidents. Hence, .Anti-lock braking systems (ABS) is preferred over conventional braking. ABS takes care of two aspects of braking, wheel lock-up and longitudinal control of the vehicle.

At present, many of the studies on the longitudinal stability of the vehicle has a more in-depth study, put forward a different stability control strategy [1]. In the previous studies, various methods and theories have been investigated. These include the PID control method with mixed slip characteristics [2], the robust predictive control method [3], the fuzzy control method [4] the model reference adaptive method [5] the neural-network control compensation for PID method [6], the SVR (support vector regression) method [7], the fractional-order control method [8],and Soc Method [9]. Recently much attention has been attracted by the usage of the PID control method. PID control has such advantages as a simple structure, good control effect and fast calculation time, robust and easy implementation [10]. Unfortunately, this method does not deal with parameter optimization and automatically adapt to the environmental factors caused by the complexity of vehicle dynamics, uncertainty of the external environments noise and the non-holonomic limitations of the vehicle [11]. To solve these difficulties, an adaptive control algorithm has received attention and been studied for this paper.

A Longitudinal controller is designed using the sliding mode control (SMC) algorithm due to its inherent capabilities to deal with nonlinearities, uncertainties and parametric variations in [12] and results show that the controller yields good transient performances at the expense of strong control signal and non-smooth movements. However, sliding model control has limited usage

[*] Majid Moavenian
Email Address: moaven@mail.um.ac.ir
10.22068/ijae.9.1.2895

[DOI: 10.22068/ijae.9.1.2895]

in practice since it requires fast switching on the input which may result in the chattering phenomenon. Thus, it has to be eliminated or alleviated as much as possible, in [13] the boundary layer theory is introduced to eliminate the chattering around the switching surface and the control discontinuity within a thin boundary layer. However, the boundary layer approach results in the degradation of tracking performance. To tackle these difficulties, integration of fuzzy logic control (FLC) and SMC with FSMC has been proposed to address the chattering reduction problem. This integration has been confirmed to be a powerful control scheme for a nonlinear system with uncertainties and disturbances [14]

In this paper, a modified adaptive fuzzy-sliding mode control (MAFSMC) approach is presented to improve the tracking performance and ensure sliding mode signal chattering reduction and accelerate the brake actuator interference. Using cooperation of CarSim / Simulink platforms for simulation of testing vehicle brake system, the stability and brake length reduction of the vehicle is confirmed, monitoring the yaw rate and slip angle.

2. Approach

The methodology used in this research has 5 steps as shown in Figure 1. In the first step state space model for the 3 DOF vehicle model shown in Figure 2 is derived based on Euler and Newton second law. In the second step, a modified SMC is designed to obtain sliding mode signal for brake actuators considering the inputs (longitudinal speed of wheels and sprung mass) and the outputs (slip angles). In step 3 brake actuators transfer function plants are identified, designing a two level Fuzzy-PID adaptive and non-adaptive, with the inputs (slip angle and master brake pressure) and output (rotor brake pressure). In step 4 the state space of vehicle dynamics, SMC, actuators and controllers are simulated in MATALB/SIMULINK in collaboration with CarSim program to test the proposed MAFSMC with 3 different proposed road conditions in step 5. The flow chart of the process is presented in Figure3.

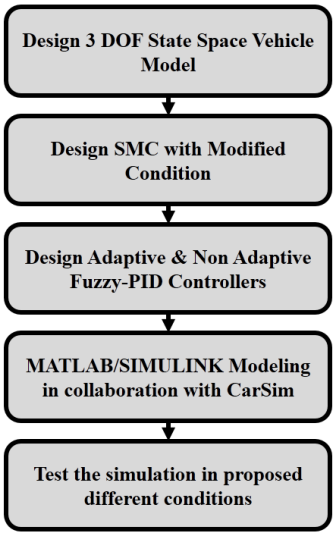

Figure 1:5 steps of methodology

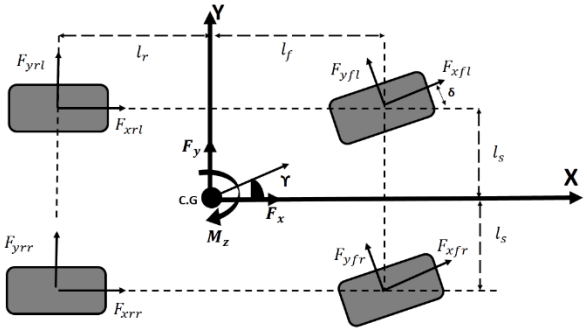

Figure 2: Schematic of vehicle model with three degrees of freedom [24]

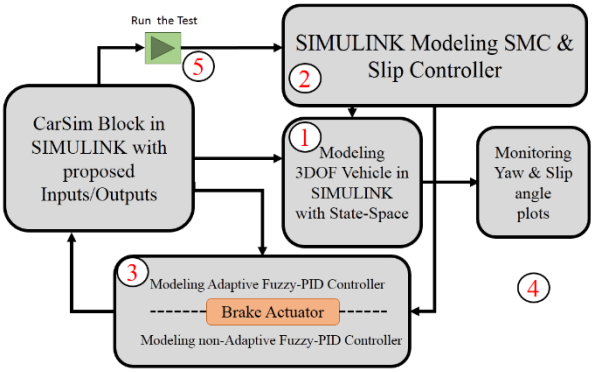

Figure3: Schematic Interconnection CarSim and MATLAB

2.1. Vehicle Model

Ignoring the pitch and roll motions, the vehicle has three planar degrees of freedom: lateral motion, longitudinal motion, and yaw motion. Figure 2, shows the schematic of the vehicle model. Where, CG is the vehicle's center of gravity. V_x , V_y are the longitudinal and lateral speeds respectively and γ is the yaw rate. Therefore, dynamic equations of

the vehicle can be expressed below as given in [15] and [16].

$$\begin{cases} M\dot{V_x} = (F_{xfl} + F_{xfr})cos\dot{\delta} - (F_{yfl} + F_{yfr})sin\delta + \\ F_{xrl} + F_{xrr} - 0.5\rho_a C_D A{V_x}^2 + MV_y\gamma \\ M\dot{V_y} = (F_{yfl} + F_{yfr})cos\delta - (F_{xfl} + F_{xfr})sin\delta + \\ F_{yrl} + F_{yrr} - MV_x\gamma \\ I_z\dot{\gamma} = (F_{yfl}sin\delta - F_{xfl}cos\delta + F_{xfr}cos\delta - F_{yfr}sin\delta) \\ l_s + (F_{xrr} - F_{xrl})l_s - (F_{yfr} + F_{yrr})l_f \\ +((F_{xfl} + F_{xfr})cos\delta + (F_{yfl} + F_{yfr})sin\delta)l_f \end{cases} \quad (1)$$

where, F_{xi} and F_{yi} (i = fl, fr, rl, rr) are respectively longitudinal and lateral forces of each tire, M is the mass of the vehicle, ρ_a is the air density, C_D is the aerodynamic drag, A is the vehicle front area, δ is the angle front wheel steering angle, and distances l_f, l_r , and l_s are shown in Fig. 2.

In (1), the steering angles of the two front wheels are assumed to be equal however in reality, these angles are approximately equal and there is a little difference between them. So, in this study, for simplicity the difference is neglected [15].

Considering (1), the state space equations of vehicle can be expressed as follows:

$$\begin{bmatrix} V_x \\ \dot{V_y} \\ \dot{\gamma} \end{bmatrix} = \begin{bmatrix} V_y\gamma - \frac{\rho_a C_D}{2M} A{V_x}^2 \\ -V_x\gamma \\ 0 \end{bmatrix} + B_y \begin{bmatrix} F_{yfl} \\ F_{yfr} \\ F_{yrl} \\ F_{yrr} \end{bmatrix} + B_x \begin{bmatrix} F_{xfl} \\ F_{xfr} \\ F_{xrl} \\ F_{xrr} \end{bmatrix} \quad (2)$$

Where B_X and B_y are:

$$B_x = \begin{bmatrix} \frac{cos\delta}{M} & \frac{cos\delta}{M} & \frac{1}{M} & \frac{1}{M} \\ \frac{sin\delta}{M} & \frac{sin\delta}{M} & 0 & 0 \\ \frac{l_f sin\delta - I_s cos\delta}{I_z} & \frac{l_f sin\delta + I_s cos\delta}{I_z} & \frac{-l_s}{I_z} & \frac{-l_s}{I_z} \end{bmatrix} \quad (3)$$

$$B_y = \begin{bmatrix} \frac{-sin\delta}{M} & \frac{-sin\delta}{M} & 0 & 0 \\ \frac{cos\delta}{M} & \frac{cos\delta}{M} & \frac{1}{M} & \frac{1}{M} \\ \frac{l_f cos\delta + I_s sin\delta}{I_z} & \frac{l_f cos\delta - I_s sin\delta}{I_z} & \frac{-l_r}{I_z} & \frac{l_r}{I_z} \end{bmatrix} \quad (4)$$

2.1.1. Tire Model

In each wheel, the traveled distance by the tire is different from the expected distance from its peripheral speed. The longitudinal slip ratio (defined as the relative difference between tire peripheral speed and tire center speed) is used to express this phenomenon [16] as:

$$S_i = \frac{\omega_i R_{eff} - V_{xi}}{\max(V_{xi}, \omega_i R_{eff})} \quad (5)$$

Where R_{eff} is the effective tire radius, ω_i is the angular speed of i-th tire, and V_{xi} is the longitudinal speed at the center of i-th wheel. The wheel speeds at the wheel centers are calculated as follows:

$$\begin{cases} V_{Xfl} = (V_x - \gamma l_s)Cos\delta + (V_y + \gamma l_f)Sin\delta \\ V_{Xfr} = (V_x + \gamma l_s)Cos\delta + (V_y + \gamma l_f)Sin\delta \\ V_{Xrl} = V_x - \gamma l_s \\ V_{Xrr} = V_x - \gamma l_s \end{cases} \quad (6)$$

The slip angle of each tire is defined as angular difference between the orientation of a wheel and the velocity of the wheel center [23]. If the tire slip angles are small, the lateral forces of tires can be calculated as [24]:

$$\begin{cases} F_{yfr} \cong F_{yfl} \cong C_f(\delta - \theta_{vf}) \\ F_{yrr} \cong F_{yrl} \cong C_r(-\theta_{vr}) \\ \tan(\theta_{vf}) = \beta + \frac{l_f\gamma}{V_x} \\ \tan(\theta_{vr}) = \beta - \frac{l_r\gamma}{V_x} \\ with\ \beta = \tan^{-1}(\frac{V_x}{V_y}) \end{cases} \quad (7)$$

Where, θ_{vf} and θ_{vr} are slip angles of front and rear tires, respectively. C_f and $C_r$are stiffness coefficients of front and rear tires, receptively, and β is the vehicle body sideslip angle.

In a vehicle, maximum applied force to a wheel is limited by the maximum capacity of the powertrain system and the friction coefficient between road and tire as (8).

$$F_{\max i} = \mu F_{zi} \quad (8)$$

Where F_{zi} is the normal load at the center of i-th wheel.

Vehicle sprung mass in a vehicle cause a load transfer during acceleration, braking and cornering conditions. The load transfer changes the normal forces of the wheel centersF_{zi}. The applied force to a wheel center can be affected by its normal force [16]. Therefore, it is required to be modeled. This phenomenon has two parts that are described as longitudinal and lateral load transfers as follow:

[DOI: 10.22068/ijae.9.1.2895]

2.1.2. Longitudinal Load Transfer

Assume, F_{zdi} (F_{zd-fl}, F_{zd-rl}, F_{zd-fr}, and F_{zd-rr}) are the tire normal forces in a standstill state or on driving with a constant speed. In (9), m is the sprung mass, h_{CG} is the height of sprung mass and m_w is the total mass of the wheel [24].

$$\begin{cases} F_{zd-f} = F_{zd-fl} = F_{zd-fr} = m_w g + \dfrac{mgl_r}{2(l_f + l_r)} \\ F_{zd-r} = F_{zd-rl} = F_{zd-rr} = m_w g + \dfrac{mgl_r}{2(l_f + l_r)} \end{cases} \quad (9)$$

In the acceleration and braking conditions, the sprung mass is moved backward and forward, respectively. Consequently, the normal forces of the wheels, during longitudinal load transfer (z_x), can be expressed as follows:

$$\begin{cases} F_{z-front} = F_{zd-f} - Z_x \\ F_{z-rear} = F_{zd-r} + Z_x \\ Z_x = \dfrac{mh_{CG}a_x}{2(l_f+l_r)} \end{cases} \quad (10)$$

2.1.3. Lateral Load Transfer

The sprung mass is moved during vehicle cornering because of centrifugal force. In this situation, the wheel's normal forces on one side of the vehicle are increased and the normal forces on the other side are reduced. Therefore, the lateral load transfer (z_y) can be expressed as follows:

$$\begin{cases} F_{zfl} = F_{zd-fl} + Z_y \\ F_{zrl} = F_{zd-rl} + Z_y \\ F_{zfr} = F_{zd-fr} - Z_y \\ F_{zrr} = F_{zd-rr} + Z_y \\ Z_y = \dfrac{mh_{CG}a_y}{4l_s} \end{cases} \quad (11)$$

Consequently, the total tire normal loads can be calculated as [16]:

$$\begin{cases} F_{zfl} = m_w g + \dfrac{mgl_r}{2(l_f + l_r)} - \dfrac{mh_{CG}a_x}{2(l_f + l_r)} - \dfrac{mh_{CG}a_y}{4l_s} \\ F_{zfr} = m_w g + \dfrac{mgl_r}{2(l_f + l_r)} - \dfrac{mh_{CG}a_x}{2(l_f + l_r)} + \dfrac{mh_{CG}a_y}{4l_s} \\ F_{zfl} = m_w g + \dfrac{mgl_f}{2(l_f + l_r)} - \dfrac{mh_{CG}a_x}{2(l_f + l_r)} - \dfrac{mh_{CG}a_y}{4l_s} \\ F_{zfl} = m_w g + \dfrac{mgl_f}{2(l_f + l_r)} - \dfrac{mh_{CG}a_x}{2(l_f + l_r)} + \dfrac{mh_{CG}a_y}{4l_s} \end{cases} \quad (12)$$

By selecting β and γ as state variables, the state space of a vehicle can be expressed as (13).Where M_z is the vehicle direct moment.

$$\begin{bmatrix} \dot{\beta} \\ \dot{\gamma} \end{bmatrix} = \begin{bmatrix} \dfrac{-2(C_f+C_r)}{MV_x} & \dfrac{2(-l_fC_f+l_rC_r)}{MV_x{}^2} \\ \dfrac{2(-l_fC_f+l_rC_r)}{I_z} & \dfrac{-2(l_f{}^2C_f+l_r{}^2C_r)}{I_zV_x} \end{bmatrix} \begin{bmatrix} \beta \\ \gamma \end{bmatrix} + \begin{bmatrix} \dfrac{2C_f}{MV_x} \\ \dfrac{2l_fC_f}{I_z} \end{bmatrix} \delta + \begin{bmatrix} 0 \\ \dfrac{1}{I_z} \end{bmatrix} M_z \quad (13)$$

2.2. Modified Conditions SMC

More than 7 decades is past since early definition and design principles of SMC is published in automatic control literatures. A new sliding mode controller was proposed by H.Alipour et al. [17] , where Lyapunov theorem is used to prove the stability. They showed that the designed sliding mode control structure was faster, more accurate and robust, with lower chatter than classic sliding mode controller. They calculated the setting time using following equation:

$$t_{set} \leq \frac{2}{k} \ln \frac{k_1}{k\lambda} \left(S_0 + \frac{k\lambda}{k_i} \right) \quad (14)$$

Note that, $t_{set(Max)}$ for classic SMC is equal to S_0/k and in [25], $t_{set(Max)}$ is reduced logarithmic with k. But in the present study the value of k is set using Genetic Algorithm method with the aim of minimizing slip angle (one of the inputs of brake actuator), the result was considerable reduction of chattering and start time of the controller activity, leading to reduction of brake distance.

2.3. Adaptive Fuzzy-PID Controllers

The brake pressures as output of the brake system, are optimized by brake actuator controllers to reduce the braking time and distance. Two inputs for brake system are selected. The first one, β_i is one of SMC outputs (the slip angle of each tire), and the second one, is P_{con} (the pedal pressure applied by the driver).

To maintain the test in a real condition, 1 minute delay is considered for driver reaction time, when 15Mpa pedal pressure is activated, as shown in Figure 4.

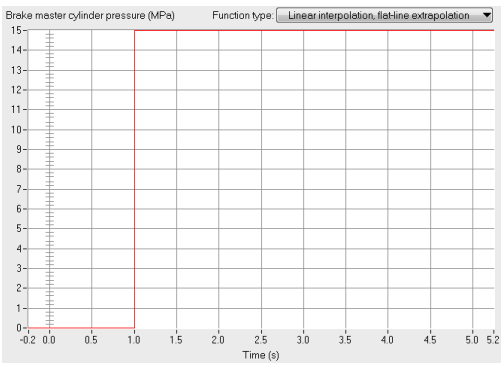

Figure 4: Pedal Brake Pressure

To obtain transfer functions for this multi-input/single-output system (MISO), MATLAB system identification toolbox was used by enforcing unit pulse $\delta(t)$ inputs and presumed non zero and 2 poles transfer function. The identified transfer function 1 (tf1) applied for SMC output, named "control mode". Also transfer function 2 (tf2) for pedal pressure (P_{con}) input. Both transfer function's outputs are brake pressure (P_{bi}) which are set in brake actuator controllers below, respectively.

$$tf1 = \frac{5.6\times10^{-5}}{s^2+0.4384\,s+0.1182} \quad (15)$$

$$tf2 = \frac{6.5\times10^{-5}}{s^2+0.8348\,s+0.212} \quad (16)$$

The brake actuator is divided into 2 controllers shown in Figure 5 and 6. Figure 5 represent Figure 3 with more details, signal connections and inputs-output of 2-Level Fuzzy-PID Controller (the MISO system) mentioned before.

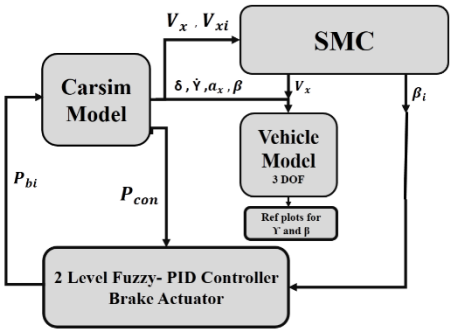

Figure5: Scheme of Simulink blocks and signals

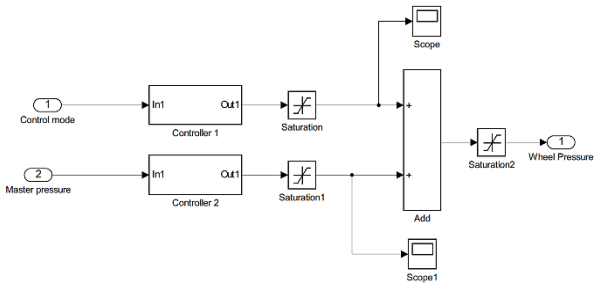

Figure6: Scheme of 2 level Fuzzy-PID controller of Brake Actuator

2.3.1. Main Level Fuzzy-PID controller

Controller 1 and 2 have two levels called Main and Inner part, their difference is only, being adaptive or non-adaptive which are defined in Figures 7 and 8.

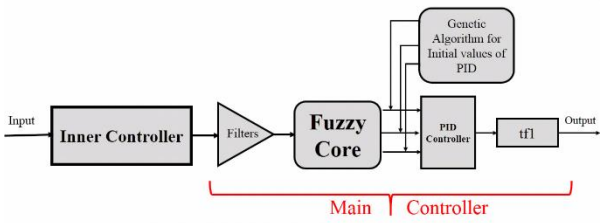

Figure7: Controller 1 scheme

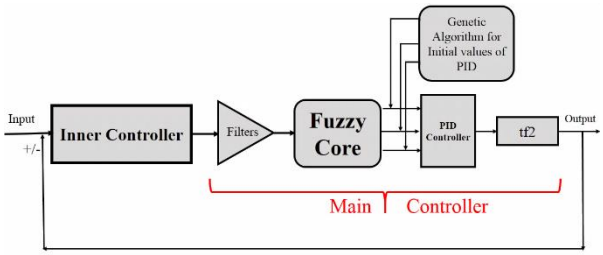

Figure8: Controller 2 scheme

The Fuzzy Core of main controller builds on having two inputs, e and e_c (error and derivative of error) and three output gains, Kp, Ki and Kd. The initial gain values Kp_0 , Ki_0 and Kd_0 for the controller are obtained by means of Genetic Algorithm as presented in Table 1. A genetic algorithm (GA) is a method for solving both constrained and unconstrained optimization problems based on a natural selection process that mimics biological evolution. The algorithm repeatedly modifies a population of individual solutions. At each step, the genetic algorithm randomly selects individuals from the current population and uses them as parents to produce the children for the next generation. Over successive generations, the population "evolves" toward an optimal solution.

The Fuzzy Logic toolbox let us model complex system behaviors using simple logic rules, and then implement these rules in a fuzzy inference system. It be can used as a stand-alone fuzzy inference engine. Alternatively, you can use fuzzy inference blocks in Simulink and simulate the fuzzy systems within a comprehensive model of the entire dynamic system.

Table1: initial values for PID controllers

Parameter	Kp_0	Ki_0	Kd_0
Value	10	0.5	1

Fuzzy rules, input and output functions used in the main controller are shown in Table2, Figure 9 and 10 respectively.

[DOI: 10.22068/ijae.9.1.2895]

Table2: Fuzzy Rules (Main Controller)

	Value	Rules
1	1	If (e is NB) then (kp is PB),(ki is ZO),(kd is PB)
2	1	If (e is NM) and (ec is NM) then (kp is PM),(ki is PS),(kd is PM)
3	1	If (e is NM) and (ec is PM) then (kp is PM),(ki is PS),(kd is PM)
4	1	If (e is NS) and (ec is NS) then (kp is PB),(ki is PB),(kd is PM)
5	1	If (e is NS) and (ec is PS) then (kp is PB),(ki is PB),(kd is PM)
6	1	If (e is PS) and (ec is NS) then (kp is PB),(ki is PB),(kd is PM)
7	1	If (e is PS) and (ec is PS) then (kp is PB),(ki is PB),(kd is PM)
8	1	If (e is PM) and (ec is NM) then (kp is PB),(ki is ZO),(kd is PS)
9	1	If (e is PM) and (ec is NM) then (kp is PM),(ki is PS),(kd is PS)
10	1	If (e is PB) then (kp is PB),(ki is ZO),(kd is PB)

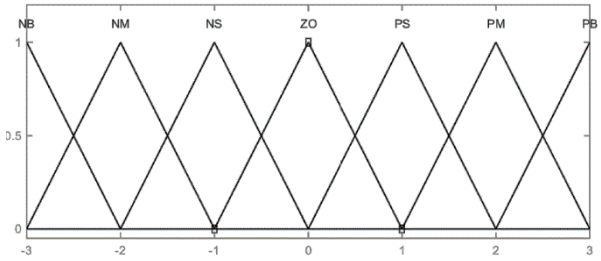

Figure9: Input functions (e ande_c)

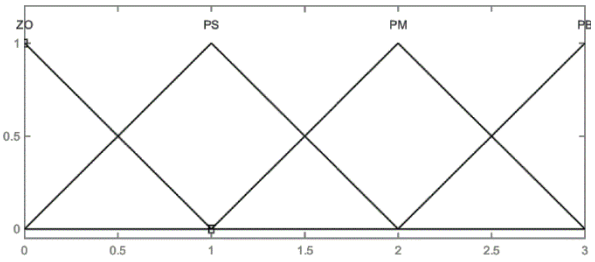

Figure10: Output functions (Ki, Kp and Kd)

2.3.2 Inner Level Fuzzy Controller

The inner controller is based on Fuzzy Core with two inputs E and E_c (error and derivative of error and three outputs). Kp, Ki and Kd (gain values) are obtained by MATLAB (optimization toolbox) as presented in table 2 below:

Table3: gain values for PID controllers

Parameter	Kp_0	Ki_0	Kd_0
Value	0.5	0.5	0.00005

The proposed Fuzzy rules, input and output function, used in the inner controller are shown in Tables 4-6 and Figures 11 and 12.

Table4: Fuzzy rules of Kp

E \Ec	NB	NM	NS	ZO	PS	PM	PB
NB	PB	PB	PM	PM	PS	ZO	ZO
NM	PB	PB	PM	PS	PS	ZO	NS
NS	PM	PM	PM	PS	ZO	NS	NS
ZO	PM	PM	PS	ZO	NS	NM	NM
PS	PS	PS	ZO	NS	NS	NM	NM
PM	PS	ZO	NS	NM	NM	NM	NB
PB	ZO	ZO	NM	NM	NM	NB	NB

Table5: Fuzzy rules (Ki)

E \Ec	NB	NM	NS	ZO	PS	PM	PB
NB	PS	NS	NB	NB	NB	NM	PS
NM	PS	NS	NB	NM	NM	NS	ZO
NS	ZO	NS	NM	NM	NS	NS	ZO
ZO	ZO	NS	NS	NS	NS	NS	ZO
PS	ZO	ZO	ZO	ZO	ZO	ZO	ZO
PM	PB	NS	PS	PS	PS	PS	PB
PB	PB	PM	PM	PM	PS	PS	PB

Table6: Fuzzy rules (Kd)

E \Ec	NB	NM	NS	ZO	PS	PM	PB
NB	NB	NB	NM	NM	NS	ZO	ZO
NM	NB	NB	NM	NS	NS	ZO	ZO
NS	NB	NM	NS	NS	ZO	PS	PS
ZO	NM	NM	NS	ZO	PS	PM	PM
PS	NM	NS	ZO	PS	PS	PM	PB
PM	ZO	ZO	PS	PS	PM	PB	PB
PB	ZO	ZO	PS	PM	PM	PB	PB

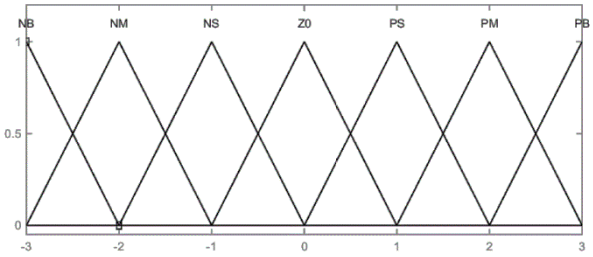

Figure11: Inputs Functions (E and E_c)

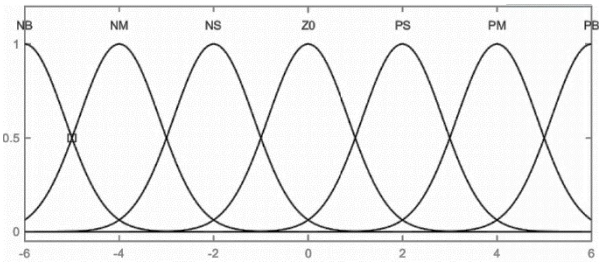

Figure12: Outputs Functions (Kp, Ki and Kd)

2.4. Simulink Modeling

Inputs and outputs for the proposed MAFSMC system in CarSim software are selected and exported into Simulink platform (MATLAB). Vehicle dynamics, SMC, Brake actuators and signal structures was shown in figure 5.

2.5. Test Conditions

The conducted experiments were carried on a chosen class of vehicle's which is available in CarSim and will be used as the test rig for all experiments. The chosen class has the following specification shown in figures 13 and 14 which can be verified by Vehicles in C-Class Hatch back like Audi A3 as an example of common familial car.[18]

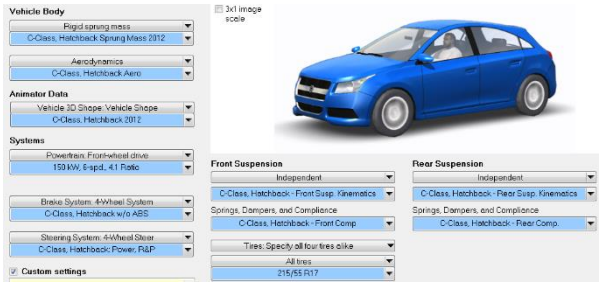

Figure13: CarSim vehicle's configuration part

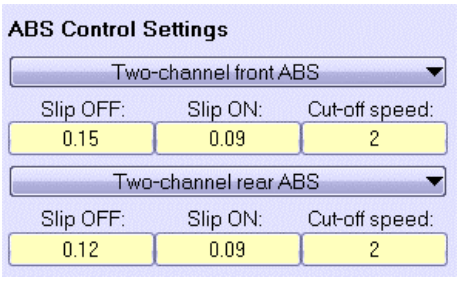

Figure14: Vehicle's ABS ON/OFF controller in CarSim

Table7: Vehicle's Parameters

Parameters	**Notation**	**Value**	**Unit**
Vehicle total mass	M	1500	kg
Vehicle Sprung mass	m	1370	kg
Roll inertia	I_{xx}	671.3	$kg.m^2$
Pitch inertia	I_{yy}	1972.8	$kg.m^2$
Yaw inertia	I_{zz}	2315.3	$kg.m^2$
Aerodynamic Drag Coefficient	C_D	0.32	-
Frontal Area	A	2.5	m^2
Air density	ρ	1.206	kg/m^3
Tire effective rolling radius	R_{eff}	0.325	m
Half of Lateral distance between centers of tire	l_s	0.85	m
Distance from the front axle to the mass center	l_f	1.1	m
Distance from the rear axle to the mass center	l_r	1.2	m
Maximum Allowable Brake Torque	T_b	500	N.m/MPa
Engine Model (for 6 speed transmission Automatic)	-	150	kW

And three road conditions (dry, wet and icy see table 8) were considered for vehicle driven in three following simulated conditions that imported manually in CarSim.

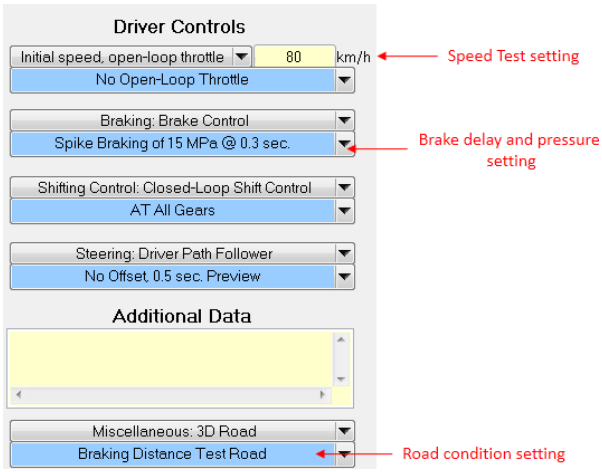

Figure 15: CarSim Test conditions procedure part

Table8: JASO (Japanese Standard Organization) Test Conditions

Road	Condition	Friction	Speed
Dry road	Dry asphalt	0.8	120 km/h
		0.8	50 km/h
Wet road	Wet asphalt	0.5	80 km/h
		0.5	50 km/h
Icy road	Icy asphalt	0.2	50 km/h

For vehicle driven in three simulated conditions; 1)"Carsim_ABS_OFF", 2)"Carsim_ABS_ON" 3) and the proposed "MAFSMC_ON" see Figure 14.

2.5. Brake Rotor Modeling

The brakes system is critical with respect to vehicle safety. One situation during which the brake system is put to the test is an Alpine descent. Such a descent causes very high brake system temperatures.Stress and Temperature distribution for FGM brake pads had been studied at [19]. The model and its specification that used in our study adapted form [20]. Which its data and modal investigated with accuracy and fits our CarSim Vehicle Model.

3. Results

In order to evaluate the test results, the first step is to check whether they are observing the standard regulation established by 'Transport Research Laboratory of UK' [21] and also stopping sight distance prepared for "Oregon Department of Transportation Salem" [22] see figures 17 and 18. Stop Distance Results for each conditions

compared to previous study [23].however a study which held test conditions for Brake rotor temperature like our study was not found and ought to just make sure they don't exceed the maximum Torque/Pressure Coefficient of pads which are 250 and 150 N.m/MPa for front and rear wheels. This can be helped by applying an "If Block" in Simulink model of Brake signal which prevent the test if overlap occurs.

Speed (km/h)	Minimum Reaction Distance (m)	Minimum Braking Distance (m)	Total Minimum Stopping Distance (m)
30	6	6	12
40	8	10	18
50	10	15	25
60	12	21	33
80	16	36	52
100	20	50	70
120	24	78	102

Source Transport Research Laboratory, UK, 2012, © Road Safety Authority, 2012.

Figure 17: Standard stop distance proposed by [26]

Design Speed (km/h)	Decision Sight Distance for Avoidance Maneuver, (meters)				
	A	B	C	D	E
50	75	160	145	160	200
60	95	205	175	205	235
70	125	250	200	240	275
80	155	300	230	275	315
90	185	360	275	320	360
100	225	415	315	365	405
110	265	455	335	390	435
120	305	505	375	415	470

Figure18: Decision sight distance for braking in different road condition [27]

Running the above tests the resulted following figures for all conditions are shown in sections 3.1 to 3.3.

3.1. Dry Road

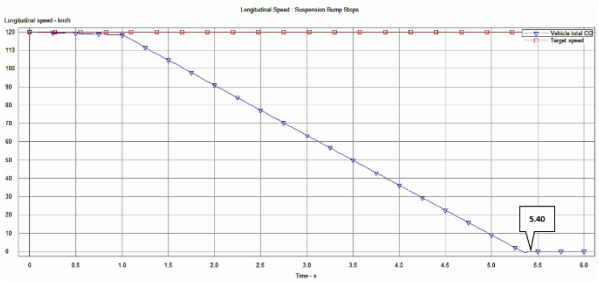

Figure20: Brake Speed km/h-Time(s)
"Carsim_ABS_OFF"

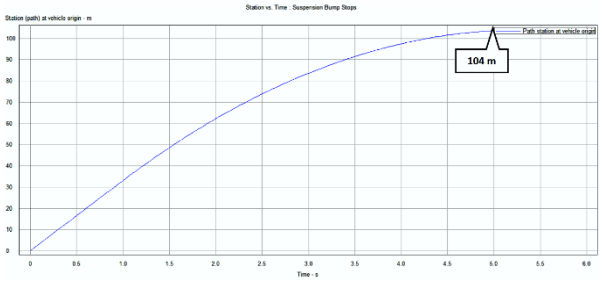

Figure21: Brake Distance m-Time(s)
"Carsim_ABS_OFF"

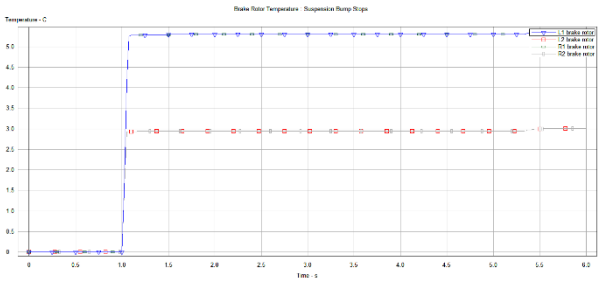

Figure22: Brake Rotor Temperature C-Time(s)
"Carsim_ABS_OFF"

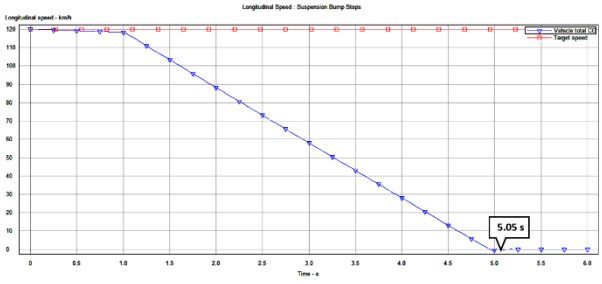

Figure23: Brake Speed km/h-Time(s)
"Carsim_ABS_ON"

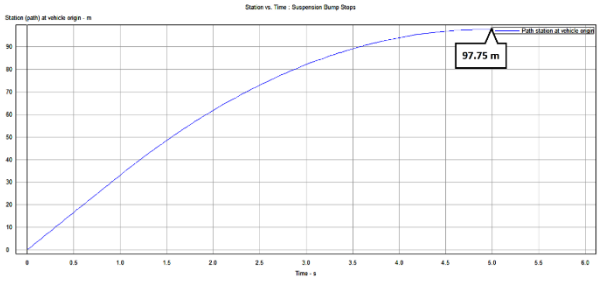

Figure24: Brake Distance m-Time(s)
"Carsim_ABS_ON"

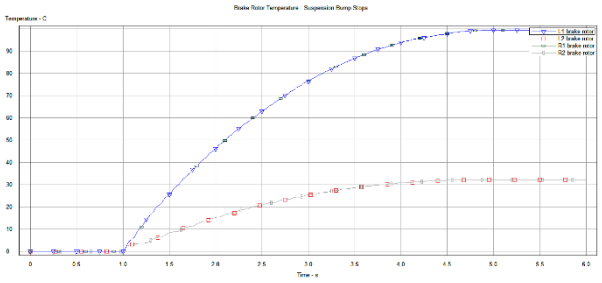

Figure25: Brake Rotor Temperature C-Time(s)
"Carsim_ABS_ON"

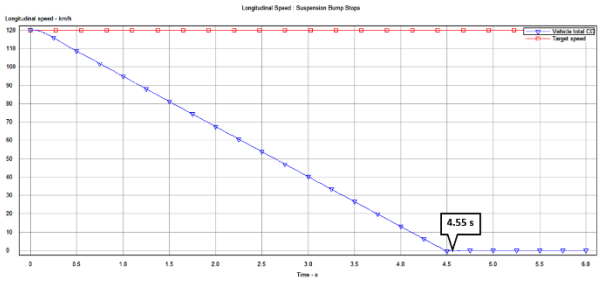

Figure26: Brake Speed km/h-Time(s)
"MAFSMC _ON"

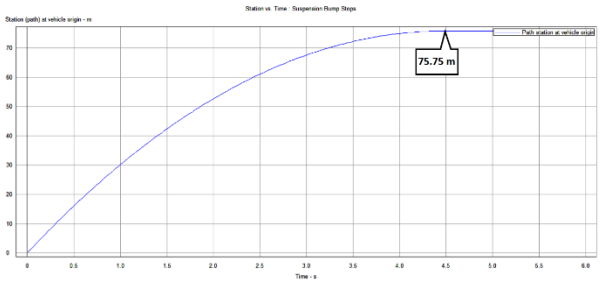

Figure27: Brake Distance m-Time(s)
"MAFSMC _ON"

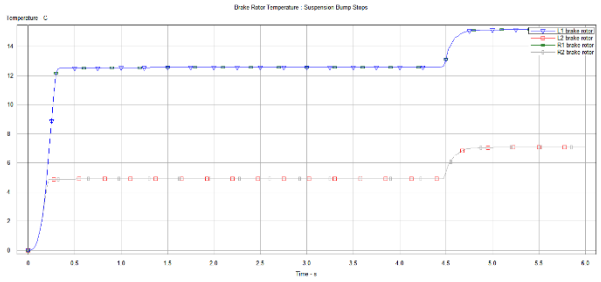

Figure28: Brake Rotor Temperature C-Time(s)
"MAFSMC _ON"

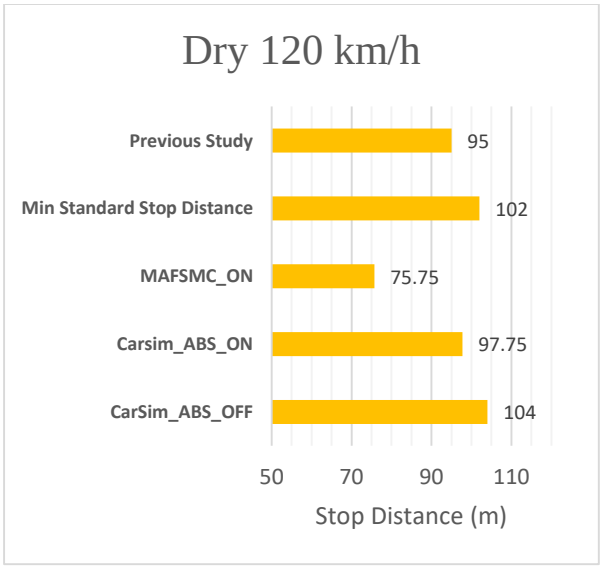

Figure29: Comparison of Brake Distance in different situations

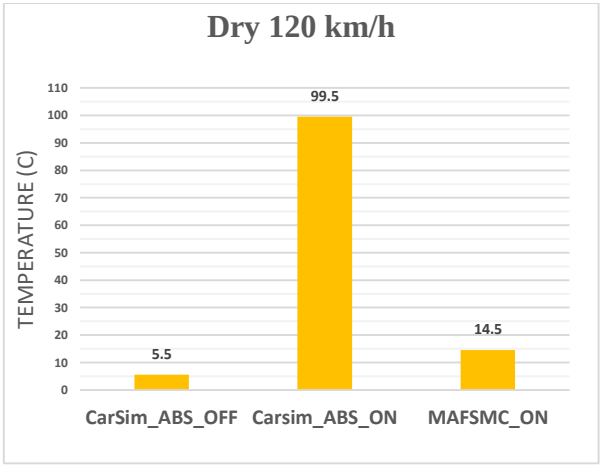

Figure30: Comparison of Brake Rotor Temperature in different situation (No exceed)

3.2. Wet Road

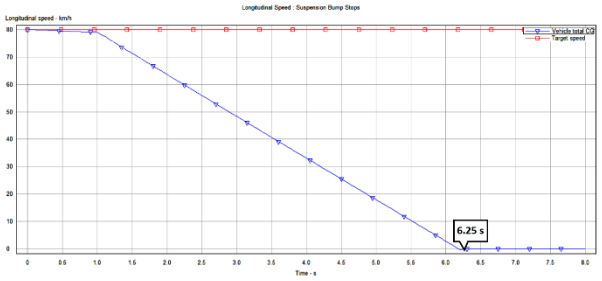

Figure31: Brake Speed km/h-Time(s)
"Carsim_ABS_OFF"

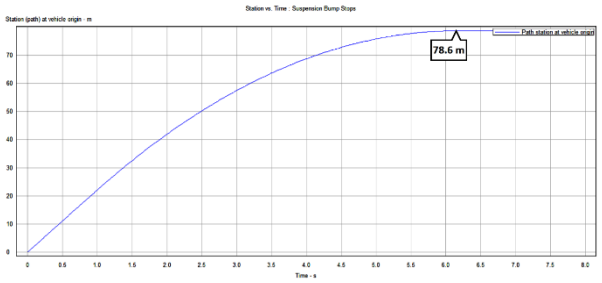

Figure32: Brake Distance m-Time(s)
"Carsim_ABS_OFF"

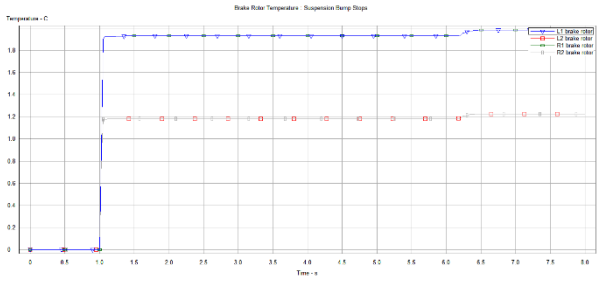

Figure33: Brake Rotor Temperature C-Time(s)
"ABS_OFF"

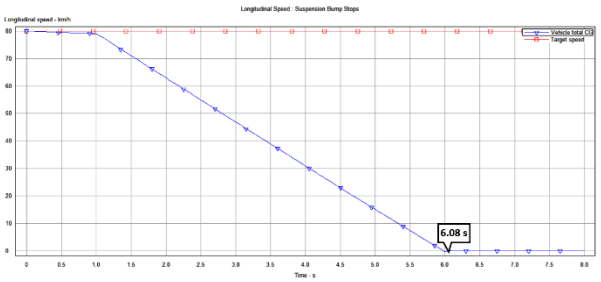

Figure34: Brake Speed km/h-Time(s) "Carsim_ABS_ON"

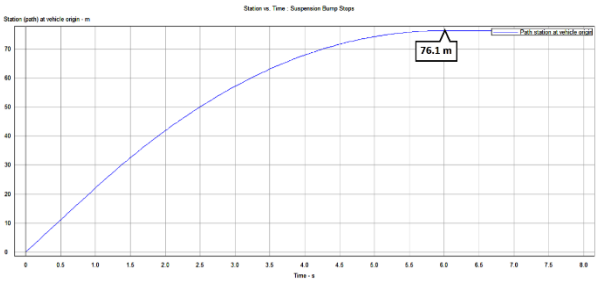

Figure35: Brake Distance m-Time(s) "Carsim_ABS_ON"

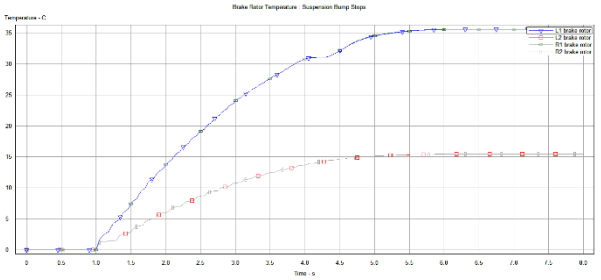

Figure36: Brake Rotor Temperature C-Time(s) "Carsim_ABS_ON"

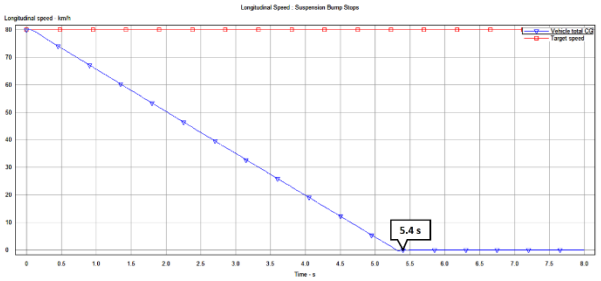

Figure37: Brake Speed m-Time(s) "MAFSMC _ON"

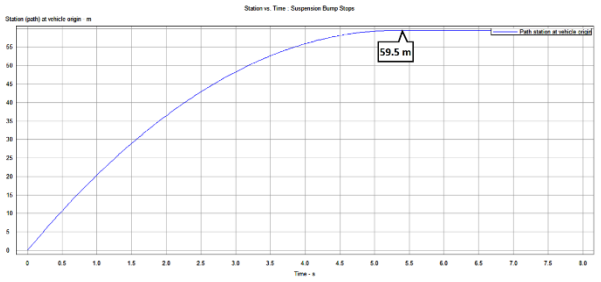

Figure38: Brake Distance m-Time(s) "MAFSMC _ON"

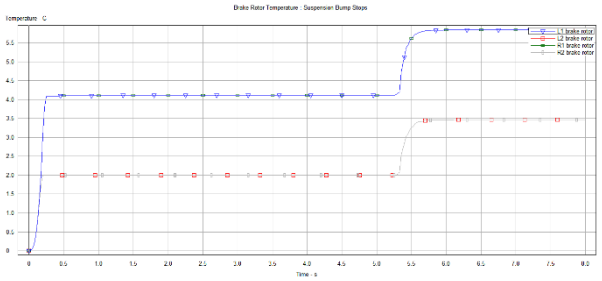

Figure39: Brake Rotor Temperature C-Time(s) "MAFSMC _ON"

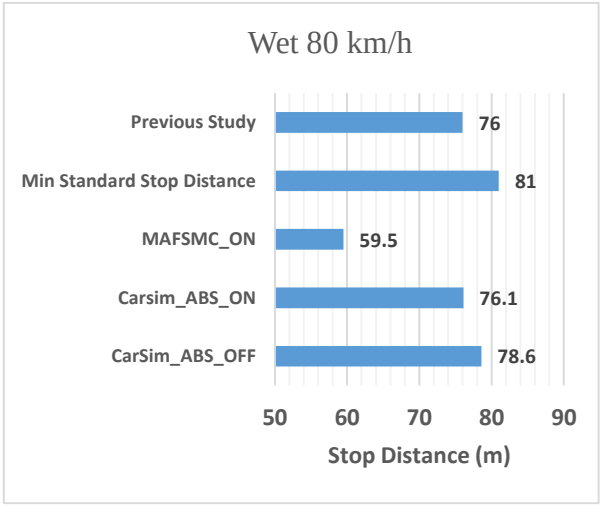

Figure40: Comparison of Brake Distance in different situations

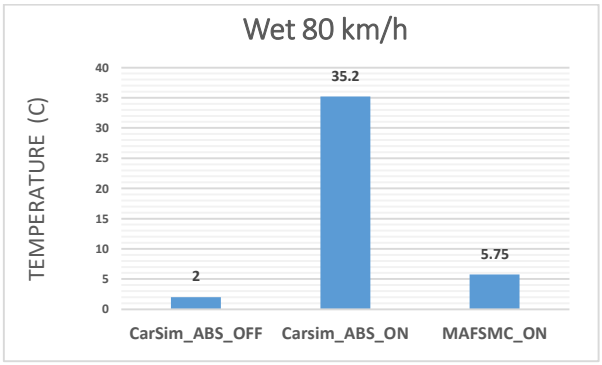

Figure41: Comparison of Brake Rotor Temperature in different situation (No exceed)

3.3. Icy Road

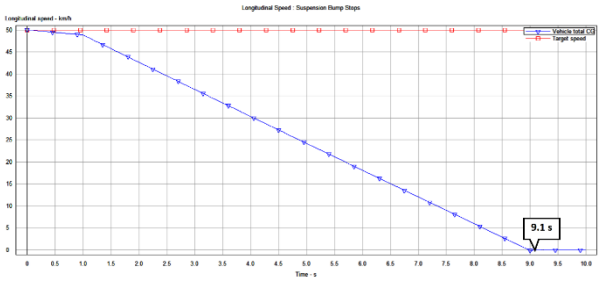

Figure42: Brake Speed km/h-Time(s) "Carsim_ABS_OFF"

[DOI: 10.22068/ijae.9.1.2895]

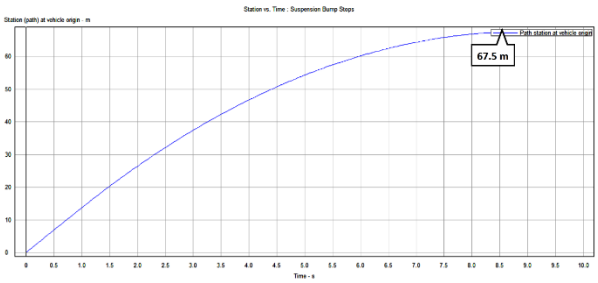

Figure43: Brake Distance m-Time(s)
"Carsim_ABS_OFF"

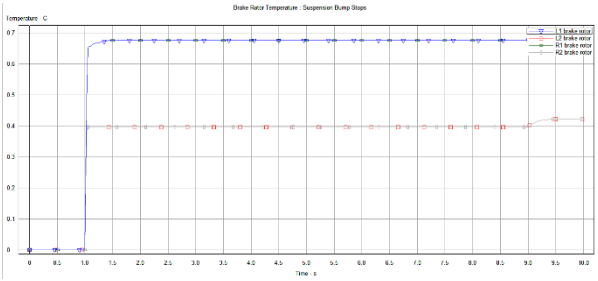

Figure44: Brake Rotor Temperature C-Time(s)
"Carsim_ABS_OFF"

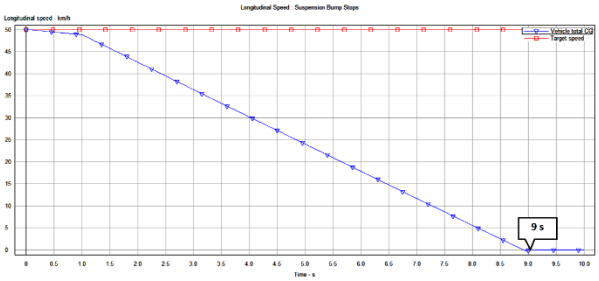

Figure45: Brake Speed km/h-Time(s)
"Carsim_ABS_ON"

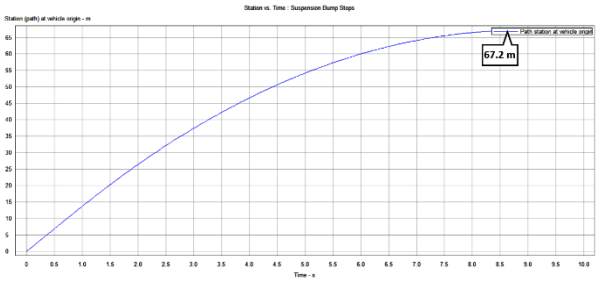

Figure46: Brake Distance m-Time(s)
"Carsim_ABS_ON"

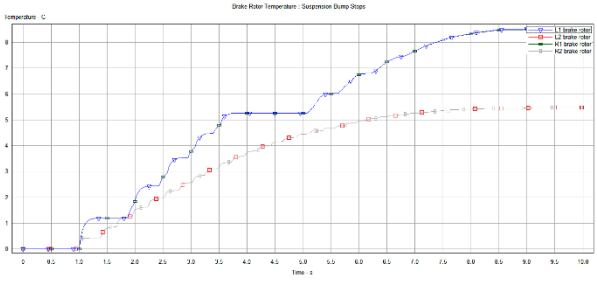

Figure47: Brake Rotor Temperature C-Time(s)
"Carsim_ABS_ON"

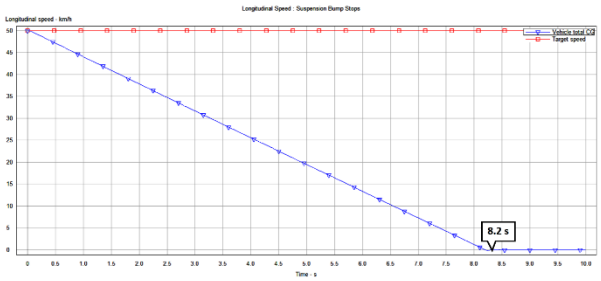

Figure48: Brake Speed km/h-Time(s)
"MAFSMC _ON"

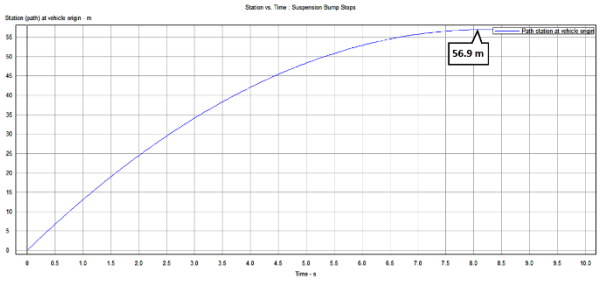

Figure49: Brake Distance m-Time(s)
"MAFSMC _ON"

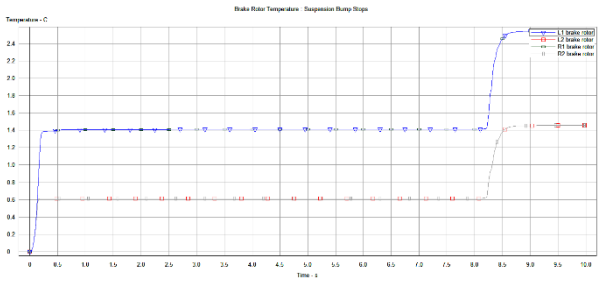

Figure50: Brake Rotor Temperature C-Time(s)
"MAFSMC _ON"

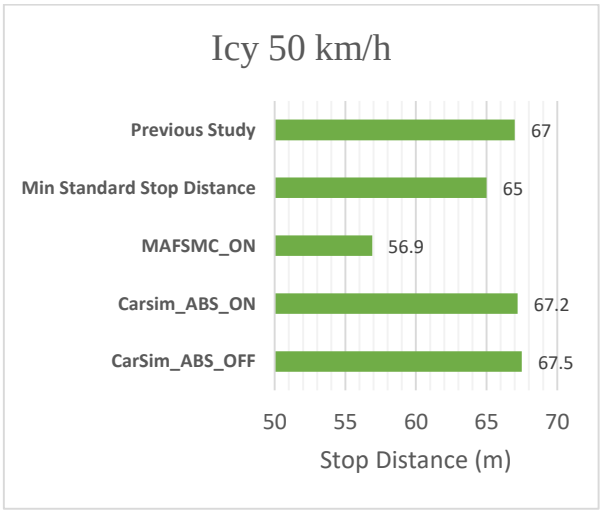

Figure51: Comparison of Brake Distance in different situations

[DOI: 10.22068/ijae.9.1.2895]

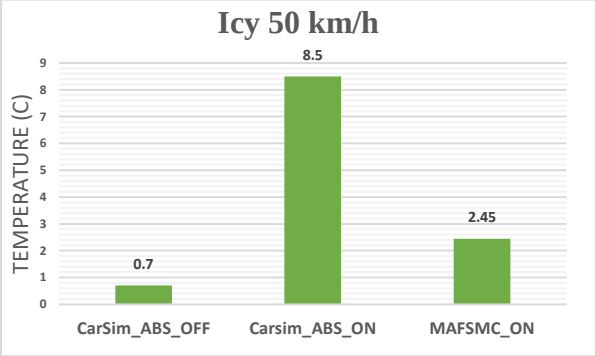

Figure52: Comparison of Brake Rotor Temperature in different situation (No exceed)

Variable	Icy Condition	Wet Condition	Dry Condition
Brake Distance Reduction	10.3 m	6.5 m	4.5 m
Brake Rotor Temperature Reduction	6.5 C	23 C	26.5 C

Table 9: Reduction of Brake Distance and Rotor Temperature in three different condition when MAFSMC_ON is replaced with traditional SMC(Carsim_ABS_ON)

4. Discussion

As it can be seen from the result figures above when comparing the brake distance, the proposed MAFSMC system reduces the distance (braking time) considerably.

Considering the results in terms of increasing brake rotor temperature although MAFSMC brake system temperature is reduced comparing with all "CarSim ABS_ON" (condition 2), but obviously when condition 1 is active the temperature is very low.

As it can be seen in Table 9 brake distance and temperature are reduced in all conditions at equal speed of 50 km/h , since the relation between friction coefficients of road and slip angle are not quite linear (Eq 1.) and slip angle as input of SMC follows a logarithmic relation, modified with Genetic Algorithm (Eq 14), the reduction percentages will not follow an exact linear function of the road friction coefficient.

Due to limitations on the required physical facilities for experiments the selected test rig in this research was chosen to be CarSim simulation software. Although CarSim is used by lots of vehicle industries as a powerful design tool, but there are some more improvements needed to make it ideal, for example in this research variation of road friction coefficients was needed for one tire, but it was not accessible through Simulink co-operation with CarSim .

5. Conclusion

In this paper, a Fuzzy Adaptive sliding mode controller for an anti-lock braking system is developed to reduce brake distance. Simulation results through running co-simulation of CarSim and MATLAB verified the vehicle has a better performance than when controlled by ABS alone.
The main achievements of this investigation can be summarized as below:

1. Accelerating ABS performance, a modified condition SMC was used to compensate the driver's delay.
2. Modifying SMC design by applying Genetic Algorithm for setting time to minimize the slip angle.
3. Using Two types of Fuzzy-PID controllers, adaptive and non-adaptive for SMC and pedal pressure, respectively were set for controlling brake actuators.
4. Verifying the performance of MAFSMC brake system designed in this paper, various road conditions with different friction settings were examined considering JASO regulation.

The results obtained show that MAFSMC brake has better performance in comparison to traditional vehicle ABS system.

References

[1] Hui-min Lia, Xiao-bo Wang. Vehicle Control Strategies Analysis Based on PID and Fuzzy Logic Control. Procedia Engineering, 2016, 137: 234 – 243.

[2] Meng Q. Chen et al.,Mixed Slip-Deceleration PID Control of Aircraft Wheel Braking System, IFAC PapersOnLine 51-4 (2018) 160–165

[3] H. Mirzaeinejad, Robust predictive control of wheel slip in antilock braking systemsbased on adial basis function neural network Applied Soft Computing 70 (2018) 318–329.

[4] Hui-min Li et al, Vehicle Control Strategies Analysis Based on PID and Fuzzy Logic ControlProcedia Engineering 137 (2016) 234 – 243.

[5] Jinghua Guo , Linhui Li , Keqiang Li & Rongben Wang (2013) An adaptive fuzzy-sliding lateral control strategy of automated vehicles

based on vision navigation, Vehicle System Dynamics: International Journal of Vehicle Mechanics and Mobility, 51:10, 1502-1517.

[6] PID Control with Intelligent Compensation for Exoskeleton Robots,Chapter5:PID Control with eural Compensation, ,2018 DOI: 10.1016/B978-0-12-813380-4.00005-0.

[7] J. Feng et al., Dynamic reliability analysis using the extended support vector regression (X-SVR) Mechanical Systems and Signal Processing 126 (2019) 368–391.

[8] Tufan Dogruer et al, Design of PI Controller using Optimization Method in Fractional Order Control System IFAC PapersOnLine 51-4 (2018) 841–846.

[9] M. Esfahanian et al. Antilock Regenerative Braking System Design for a Hybrid Electric Vehicle, International Journal of Automotive Engineering, Vol.8, No. 3, (2018), 2769-2780.

[10] Visioli, A. (2006). Practical PID Control. Springer Verlag Advances in Industrial Control Series.

[11] Barton M. (2001) Controller development and implementation for path planning and following in an autonomous urban vehicle. Undergraduate thesis, University of Sydney, Sydney, Australia.

[12] Z. Sun et al, Nested adaptive super-twisting sliding mode control design for a vehicle steer-by-wire system. Mechanical Systems and Signal Processing 122 (2019) 658–672.

[13] R. Karve, D. Angland, T. Nodé-Langlois, An analytical model for predicting rotor broadband noise due to turbulent boundary layer ingestion, Journal of Sound and Vibration (2018), doi: 10.1016/j.jsv.2018.08.020.

[14] X. Ma et al. Cornering stability control for vehicles with active front steering system using T-S fuzzy based sliding mode control strategy, Mechanical Systems and Signal Processing (2018)

[15] Wang R, Wang J. Fault-tolerant control with active fault diagnosis for fourwheel independently driven electric ground vehicles. IEEE Trans Veh Technol 2011;60(9):4276–87.

[16] Rajamani R. Vehicle dynamics and control. 2nd ed. Springer; 2012.

[17] Alipour H et al. Lateral stabilization of a four wheel independent drive electric vehicle on slippery roads. Mechatronics (2014), http://dx.doi.org/10.1016/j.mechatronics.2014.08.006

[18] Audi A3 Specification Manual, AUDI AG, Auto-Union-Strasse 185045 Ingolstadt www.audi.com, Valid from June 2016 ,Printed in Germany, 633/1153.32.24

[19] P. Hosseini Tehrani and M.Talebi, Stress and Temperature Distribution Study in a Functionally Graded Brake Disk, International Journal of Automotive Engineering Vol. 2, Number 3, July 2012

[20] ADRIAAN NEYS, In-Vehicle Brake System Temperature Model, Master Thesis in the Master's programme in Automotive Engineering, Department of Applied Mechanics CHALMERS UNIVERSITY OF TECHNOLOGY Göteborg, Sweden, 2012.

[21] Transport Research Laboratory,UK,2018

[22] Transportation Research Institute Oregon State University Corvallis, Oregon 97331-4304, STOPPING SIGHT DISTANCE AND DECISION SIGHT DISTANCE.

[23] DukSun Yun et al, Brake Performance Evaluation of ABS with Sliding Mode Controller on a Split Road with Driver Model, INTERNATIONAL JOURNAL OF PRECISION ENGINEERING AND MANUFACTURING Vol. 12, No. 1, pp. 31-38

[DOI: 10.22068/ijae.9.1.2895]